

Use of Ultrafiltration Membranes for the Separation of TiO₂ Photocatalysts in Drinking Water Treatment

Soo-Ah Lee,[†] Kwang-Ho Choo,[‡] Chung-Hak Lee,^{*,†} Ho-In Lee,[†] Taegwhan Hyeon,[†] Wonyong Choi,[§] and Heock-Hoi Kwon^{||}

School of Chemical Engineering, Seoul National University, Seoul 151-742, Korea, and Division of Architectural, Civil, and Environmental Engineering, Taegu University, Kyungsan, Kyungpook 712-714, Korea, and School of Environmental Engineering, Pohang University of Science and Technology, Pohang 790-784, Korea, and Department of Chemical and Environmental Engineering, Soongsil University, Seoul 156-743, Korea

This study investigated the ability of cross-flow ultrafiltration (UF), combined with photocatalytic reactions, to separate TiO₂ photocatalysts from treated water in photocatalytic drinking water treatment. The effect of natural organic matter (i.e., humic acids) and cross-flow velocities on UF fluxes and organic removal was explored with and without UV irradiation in the photocatalytic reactor. The interaction between the two solutes in the system, humic acids and TiO₂ photocatalysts, played a significant role in the formation of dense cake layers at the membrane surface, leading to a greater flux decline during ultrafiltration of TiO₂ particles. According to visual observations of the used membranes and the estimation of back-transport velocities of the solutes, a substantial amount of TiO₂ deposited on the membrane induces more humic acids to accumulate at the membrane through the adsorption of humic acids onto TiO₂ particles. The humic-acid-laden TiO₂ particles offered more than four times higher specific cake resistance with a substantially increased compressibility coefficient than TiO₂ particles alone. The higher the cross-flow velocities, the greater the UV₂₅₄ removal achieved. This was because the rise of cross-flow velocities contributed to the reduction of concentration polarization at the membrane surface, thereby resulting in a decrease of the driving force for humic acids to pass through the membrane. When photocatalytic reactions took place with UV illumination, UV₂₅₄ removal efficiencies of the permeate were improved markedly, and also the permeate flux was kept at a constant level without any sign of fouling. Although humic acids were not completely mineralized by photocatalysis, the degradation of the humic acids helped to enhance the UF flux, as they were transformed to less adsorbable compounds.

Introduction

A photocatalytic degradation technique with TiO₂ is one of the most promising methods for the treatment of refractory organic contaminants in water and wastewater.¹ This is because the technique makes it possible for organic contaminants to be easily removed at ambient temperature and pressure.² When TiO₂ is illuminated with UV light of suitable wavelengths, charge carriers (i.e., electrons and holes) at the TiO₂ surfaces are generated, which can reduce or oxidize various organic and inorganic substances.^{3–7} In particular, halogenated derivatives of alkanes, alkenes, or aromatic compounds were found to undergo almost complete mineralization by the TiO₂-mediated photocatalytic degradation, being transformed to CO₂ and mineral acids.^{8,9} However, the rate of tetrachloroethene decomposition decreased in the presence of humic acids, which could be attributed to their scavenging of photoinduced surface oxidants. Humic acids were found to scavenge both the oxidative and reductive species,¹⁰ whereas the addition of humic acids seemed to significantly promote

the reduction of nitrate to nitrite.¹¹ The organic substances, such as fulvic and humic acids, can also alter the photodegradation pathways during the photocatalytic treatment of surface water and wastewater. On the other hand, photocatalysis with TiO₂ has recently been tested as an alternative disinfection method, reducing the formation of disinfection byproducts in drinking water treatment compared with chlorination.^{12,13}

Although TiO₂ is known to be an excellent photocatalyst for removal of organic contaminants, the separation of TiO₂ particles creates another problem to be solved in practical applications of the process.⁴ A major difficulty in the separation of TiO₂ particles from treated water arises because TiO₂ particles are too fine to be removed by gravity settling. Other investigators have reported that the separation problem can be overcome by attaching the catalysts to a suitable substrate,⁴ but in that case, the effective surface area of the TiO₂ particles will be decreased. In fact, it was reported that TiO₂ particles in suspension have a better efficiency than immobilized ones.⁵

Recently, some attempts have been made to effectively separate TiO₂ photocatalysts, for example, by coagulation, membrane separation, etc. When a coagulation technique was applied using aluminum chloride, TiO₂ particles were flocculated and settled rapidly. The TiO₂ particles were recovered from the sediment but needed several further treatment steps prior to reuse.² The

* Corresponding author. Tel.: 82-2-850-7075. Fax: 82-2-888-1604. E-mail: leech@snu.ac.kr.

[†] Seoul National University.

[‡] Taegu University.

[§] Pohang University of Science and Technology.

^{||} Soongsil University.

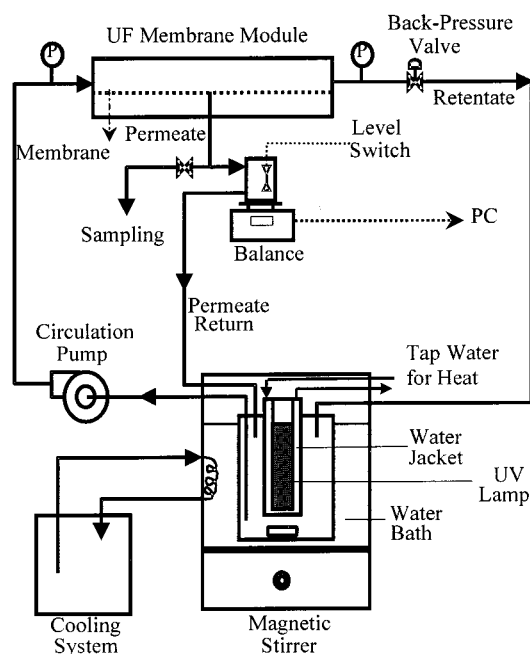


Figure 1. Schematic of a lab-scale photocatalysis/ultrafiltration system.

coagulation method also has another problem related to the production of chemical sludge that must be disposed. Another investigator tried to use a photocatalytic membrane reactor for the degradation of toxic organic species such as 4-nitrophenol while immobilizing TiO_2 particles on different flat polymeric membranes.⁶ Almost complete degradation of the organic pollutant was achieved after 5 h of irradiation, but the membranes used were slightly damaged by UV irradiation depending on the membrane materials. Other researchers tried several different approaches using a batch-recirculated photoreactor with a hollow fiber ultrafiltration membrane unit to treat methylene blue.^{14,15} They tried to examine the effect on the permeate flux of various operating parameters, such as TiO_2 dose, transmembrane pressure, and circulation rate. However, the interaction between the TiO_2 particles and the organic contaminants or membranes was not studied with respect to membrane permeability and the effect of such parameters on the removal of contaminants.

The purpose of this work was to examine the performance of UF membranes for the separation of TiO_2 photocatalysts from drinking water. In particular, the influence of operating conditions and photocatalysis on membrane permeability and natural organics removal was evaluated in depth using a lab-scale photocatalytic membrane reactor, concentrating on (1) the effect of humic acids and their interaction with TiO_2 on flux without UV irradiation, (2) the effect of cross-flow velocities on the quality of UF permeate, and (3) the removal of humic acids by photodegradation and its effect on the flux and permeate qualities.

Experimental Section

Photocatalysis/UF System. Figure 1 shows a schematic diagram of the experimental setup, which consists of a cross-flow ultrafiltration module and a photocatalytic reactor. The configuration of the UF unit was plate-and-frame. The membranes used were of the type

cellulose acetate (CA) UF (Millipore Co., Bedford, MA) with a nominal molecular weight cutoff of 30 000 Da and an effective surface area of 26.85 cm^2 . The flux was continuously measured using a balance and recorded on an on-line personal computer. After measurement, the permeate was returned to the photocatalytic reactor in order to keep the reactor volume constant. Cross-flow velocities were controlled by adjusting the pumping rate (i.e., circulation flow rate), and transmembrane pressures were regulated with a back-pressure valve. The cross-flow velocities were changed from 0.25 to 1.0 m/s, corresponding to a change in flow conditions from laminar to turbulent, and the transmembrane pressure was maintained at 1.0 ± 0.1 bar.

The photocatalytic reactor was composed of three compartments, namely, an inner chamber, an outer chamber, and a void space between them. A UV light source was placed in the inner chamber of the reactor. The outer chamber can hold 2 L of liquid for the photocatalytic reaction. During the experimental runs, tap water was continuously passed through the void space to prevent the reactor from being overheated by UV illumination. The temperature of the liquid was kept at 20 ± 2 °C by another heat exchanger along the circulation line. P-25 TiO_2 particles (Degussa, Frankfurt, Germany) were used as photocatalysts for the experiments. The suspension was irradiated using a 450-W Hg lamp (KeumKang Industry, Seoul, Korea).

Preparation of Feedwater. Stock solution [approximately 100 mg/L of dissolved organic carbon (DOC)] was first prepared by dissolving humic acid salts (Aldrich Co., Milwaukee, WI) in pure water, filtering the solution through a 0.45- μm filter, and then storing the filtrate in a refrigerator. Prior to each run, the simulated feedwater containing 4.0 ± 0.2 mg/L DOC was prepared by appropriate dilution of stock solution with addition of 50 mg/L hardness and adjustment of the pH to 7.0 with sulfuric acid. The exact DOC concentration was measured at each preparation. TiO_2 (1.0 g) was added to 2 L of the feedwater to prepare a mixture of humic acids and TiO_2 particles, and then sonication of the mixed solution was provided for 5 min before operation of the membrane unit.

Analytical Methods. The UV absorbance at 254 nm and the TOC concentration were measured using a spectrophotometer (DU-65, Beckman, Fullerton, CA) and a total organic carbon analyzer (DC-180, Dohrman, Cincinnati, OH). The concentration of TiO_2 in the permeate was measured by ICP analysis. Particle size distributions for the TiO_2 slurry and a mixture of TiO_2 and humic acids were analyzed based on a laser scattering method using a particle size analyzer (MasterSizer/E, Malvern, Worcester, U.K.). The molecular weight distribution of humic acids was analyzed using a gel permeation chromatograph (GPC, Waters, Milford, MA) equipped with GPC columns (Shodex-Ohpak, KB 802 and 803, Showa Denko K.K., Tokyo, Japan) and a refractive index detector (RID, Waters R401, Milford, MA). Poly(ethylene oxide) (SE-150, Tosoh, Tokyo, Japan) was used as a standard for calibrations.

The specific cake resistances for TiO_2 slurry and the mixtures were measured using a stirred cell unit (Amicon 8200, Beverly, MA) in an unstirred mode. Because the gravitational settling of TiO_2 particles can cause experimental errors during the measurement of the specific cake resistance, the cake layers were first formed at 0.3 bar through the filtration of 100 mL of

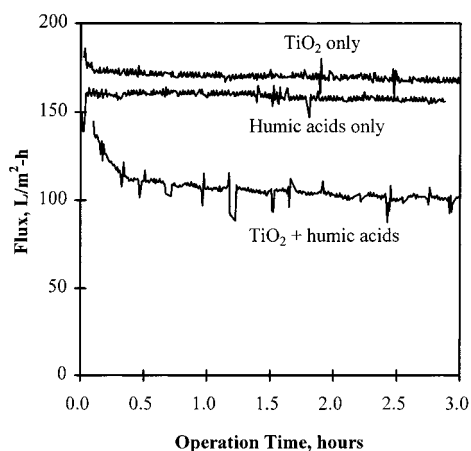


Figure 2. UF flux vs operating time with different combinations of TiO_2 and humic acids; TiO_2 concentration = 0.5 g/L, humic acids concentration = 4.0 mg/L, transmembrane pressure = 0.7 bar, cross-flow velocity = 1.0 m/s.

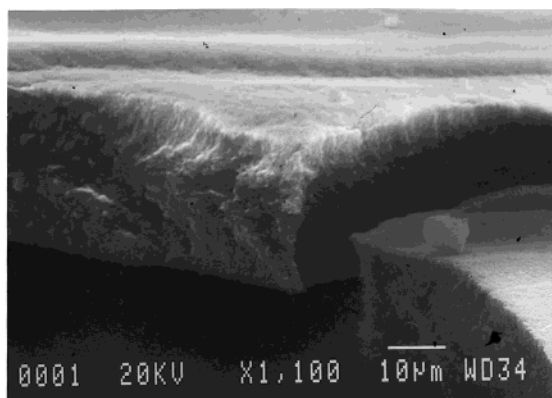
0.5 g TiO_2 /L slurries or mixtures, and then the total filtration resistance was measured at various pressures. Finally, the specific cake resistance was calculated by subtracting the membrane resistance from the total filtration resistance. On occasion, the cake layers and the membrane surfaces were visualized by a scanning electron microscope (SEM) (JSM-35, JEOL, Tokyo, Japan).

Results and Discussion

Flux Decline Due to the Interaction between Humic Acids and TiO_2 Particles. Without UV ir-

radiation, the filtration characteristics during UF of various combinations of feed solution were studied to examine the interactions among membranes, humic acids, and TiO_2 particles. Figure 2 compares UF fluxes for different combinations of feed solutions such as TiO_2 slurry alone, humic acid solution alone, and a mixture of TiO_2 and humic acids. When UF was carried out with TiO_2 slurry or humic acids alone, the fluxes remained nearly constant at an initial level of approximately 160 and 170 $\text{L m}^{-2} \text{h}^{-1}$, respectively. However, when TiO_2 particles and humic acids were mixed together, there was a noticeable flux decline from 145 to 101 $\text{L m}^{-2} \text{h}^{-1}$ (corresponding to a reduction of approximately 30%) during the first 0.5 h of operation. This was an unexpected phenomenon because the sorption of humic acids onto TiO_2 particles was anticipated to improve membrane flux or at least to keep the flux at the same level compared to that of each single-component system.

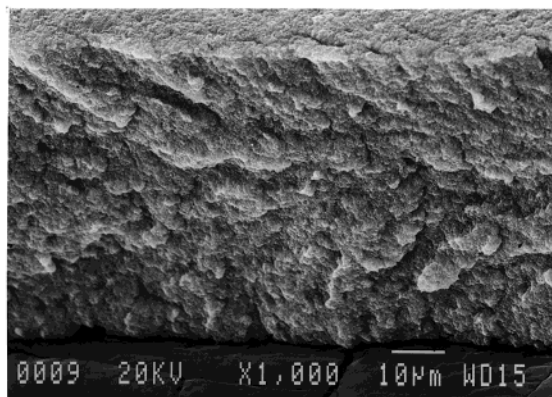
To investigate the reasons for the unexpected phenomenon, the surfaces of the UF membranes after filtration were visualized using a SEM. Figure 3 shows the deposited layers on the membrane surface after UF of the three different feed solutions. A direct comparison of the thickness between the cake layers obtained from the mixture (Figure 3a) and from TiO_2 alone (Figure 3b) cannot be made because part of the cake layer was removed when the membrane module was disassembled prior to the SEM analysis. A thick cake layer of TiO_2 particles was formed on the membrane surface when the mixture and TiO_2 alone were filtered (Figure 3a,b), whereas a very thin deposition layer of humic acids was formed with the solution of humic acids alone (Figure 3c,d). This indicates that the deposition of TiO_2 and/or



(a)



(c)



(b)



(d)

Figure 3. SEM pictures of deposition layers formed on the membrane surfaces during UF of (a) a mixture of TiO_2 and humic acids, (b) TiO_2 slurry alone, (c) and (d) humic acids alone at the different magnifications $\times 1000$ and $\times 10\,000$.

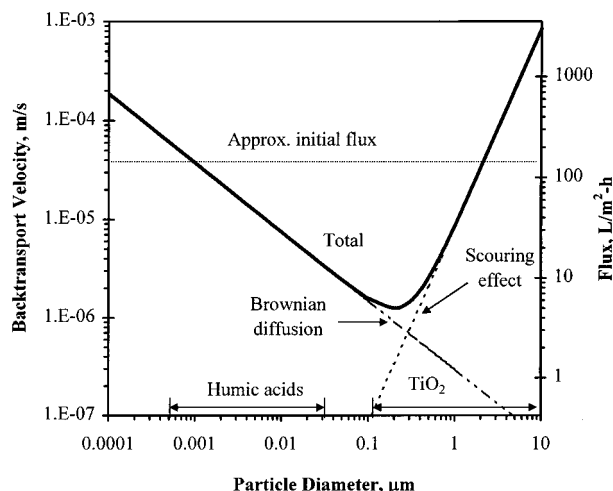


Figure 4. Back-transport velocities of particles as a function of size; cross-flow velocity = 1.0 m/s, temperature = 20 °C.

humic acids always occurs in both single- and binary-component systems during UF, even though the amounts and morphologies of the deposited layers might differ. In particular, the lack of flux decline with TiO_2 alone reveals that the cake layer of TiO_2 particles was so porous that it could not provide a perceptible flux decline. Therefore, the flux decline for a mixture of TiO_2 and humic acids was believed to be closely associated with the change in nature of the deposited layers because of the interaction between the TiO_2 particles and the humic acids. Actually, the apparent structure of the cake layer of the mixture looked somewhat denser than that of TiO_2 alone, as shown in Figure 3.

Theoretical Approach to the Deposition of TiO_2 and/or Humic Acids. To evaluate the deposition of TiO_2 particles and humic acids on the membrane surface, the back-transport velocities of solutes were computed as a function of their size under the hydrodynamic conditions studied in this work.^{16,17} The back-transport of particles from the membrane is affected by the following mechanisms: Brownian diffusion, shear-induced diffusion, lateral migration, and scouring. (1) Brownian diffusion due to the concentration gradient is caused by the interactions between the particles and the liquid, so the particles present in the polarized layer near the membrane surface are moved back to the bulk solution. (2) Shear-induced diffusion of particles occurs because of the interaction between the particles in the polarized layer and the fluid stream as one particle tumbles over another. (3) A lateral migration of particles due to inertial lift arises from nonlinear interactions of a particle with the surrounding flow field under given conditions. (4) A scouring effect comes into play when the flow regimes are unsteady, such as for turbulent flows, disturbing the formation of a concentration polarization layer. Figure 4 shows back-transport velocities calculated with the range of sizes of TiO_2 particles and humic acids used. In Figure 4, only Brownian diffusion and scouring effects were considered for the calculation, and the other factors were ignored as the flow conditions were in a turbulent region at a cross-flow velocity of 1.0 m/s. The size of the TiO_2 particles measured was in the range of 0.1–10 μm in diameter and that of the humic acids was estimated to be in the range of (5×10^{-4}) – (3×10^{-2}) μm in diameter. The estimated diameter (d_p) of the humic acids was obtained from the measurement of a molecular weight

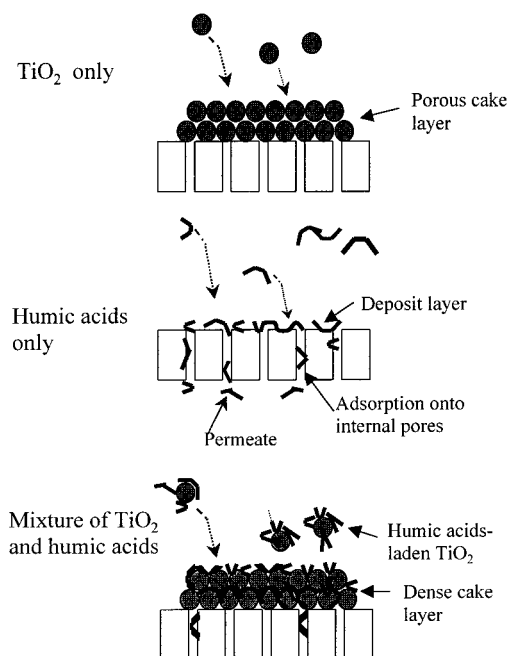


Figure 5. Illustration of possible mechanisms for the formation of deposit/cake layers at the membrane surface during UF of different combinations of solutes.

(MW) distribution by GPC and eqs 1 and 2.¹⁸ In particular, eq 2, which is based on the Einstein–Stokes theory, was adopted for the conservative estimate of the size of the humic acids in this study, although it was understood that the shape of the particles should be considered spherical.

$$D \text{ (m}^2\text{/s)} = 9.82 \times 10^{-9} (\text{MW})^{-0.52} \quad (1)$$

$$D = \frac{k_B T}{3\pi\mu d_p} \quad (2)$$

where D is the diffusivity of particle ($\text{m}^2\text{/s}$), MW is the molecular weight (Da), k_B is the Boltzmann constant (J/K), T is the absolute temperature (K), μ is the viscosity of solution (Pa s), and d_p is the particle diameter (m).

As shown in Figure 4, the particles with back-transport velocities lower than the permeate flux would be deposited onto the membrane surface as the UF flux decreased to the steady-state level, which is equal to the lowest back-transport velocity of particles present in the feed. Initially, the TiO_2 particles and humic acids that have back-transport velocities lower than approximately 4×10^{-5} m/s would be urged to move onto the membrane surface by permeation and would form cake layers on the membrane surface (Figure 3). Consequently, the permeate flux would continuously decrease until it reached its steady-state level. However, the theoretical understanding of the deposition of each solute is not yet sufficient to explain why the flux decline occurred when the two components, TiO_2 and humic acids, were mixed together.

Fouling Mechanisms for a Mixed TiO_2 /Humic Acid System. Figure 5 illustrates possible mechanisms of membrane fouling for systems with different combinations of components in the feed. TiO_2 particles or humic acids can be deposited or sorbed on the membrane surface during permeation when they exist as single components. However, when they are mixed

Table 1. Comparison of Filtration Resistances between TiO₂ Only and the Mixture

resistance ^a	TiO ₂ only ^b	mixture ^b
R_m (m ⁻¹)	1.48×10^{12} (93%)	1.36×10^{12} (59%)
R_d (m ⁻¹)	0.11×10^{12} (7%)	0.94×10^{12} (41%)

^a R_m = membrane resistance. R_d = deposition layer resistance.

^b Quantities in parentheses represent percentages of the total resistance, $R_m + R_d$.

together, humic acids can be sorbed onto the surfaces of TiO₂ particles that are either in suspension or in the cake layer. Moreover, the humic acids can occupy the vacancies between the TiO₂ particles. A portion of the deposition layer resistance actually increased when the TiO₂ particles and humic acids were mixed together, as shown in Table 1. Thus, the humic-acid-laden TiO₂ particles can be expected to give rise to a greater resistance to permeation when they form a deposition layer at the membrane surface. The above hypothesis has several important implications with respect to membrane fouling. First, a larger amount of humic acids can be deposited onto the membrane surface through the deposition of humic-acid-laden TiO₂ particles that can move to the membrane surface more easily than humic acids alone. Second, the nature of a cake layer composed of humic acids and TiO₂ particles should be denser than that of the TiO₂-only cake layer, because humic acids can exist in the void space of the TiO₂ particle layers in the mixed system.

To confirm the above hypothesis, additional investigations on the sorption of humic acids by TiO₂ and the nature of the cake layers were conducted. To evaluate the sorption properties of humic acids on TiO₂ particles, adsorption isotherm tests were performed, and the results are shown in Figure 6a. At an equilibrium DOC concentration of 2.0 mg/L, the adsorption capacity is estimated to be approximately 5.1 mg of DOC/g of TiO₂, suggesting that TiO₂ has nearly half the adsorption capacity of powdered activated carbon in a similar system, as reported elsewhere.^{19,20} In addition, to determine whether any change in the properties of the cake layers occurred in the mixed system, the specific cake resistances at different applied pressures were measured and compared with those from the TiO₂-only system (Figure 6b). The specific cake resistance of the mixture (3.8×10^{13} m/kg at 0.7 bar) was more than four times higher than that of TiO₂ alone (8.7×10^{12} m/kg). Furthermore, the compressibility coefficient for the mixture (0.94, which was obtained from the slope of a plot of the specific cake resistance versus pressure) was much larger than that of TiO₂ alone (0.39), which indicates that the cake layer of the mixture is much more compressible, so that it can cause an increase in cake layer resistance more readily when the applied pressure increases.

Effect of Cross-Flow Velocities. The effect of cross-flow velocities on the flux during UF of the mixed feed was examined without UV irradiation, and the removal efficiencies for the humic acids were simultaneously monitored. The flow conditions through the membrane channel were changed stepwise from laminar (0.25 m/s) to transition (0.64 m/s) to turbulent (1.0 m/s) flow, and the sequence was reversed from turbulent to laminar, as shown in Figure 7. UF operation started at a flux of approximately 250 L m⁻² h⁻¹, and then the flux decreased continuously to 88 L m⁻² h⁻¹ during the 6-h run,

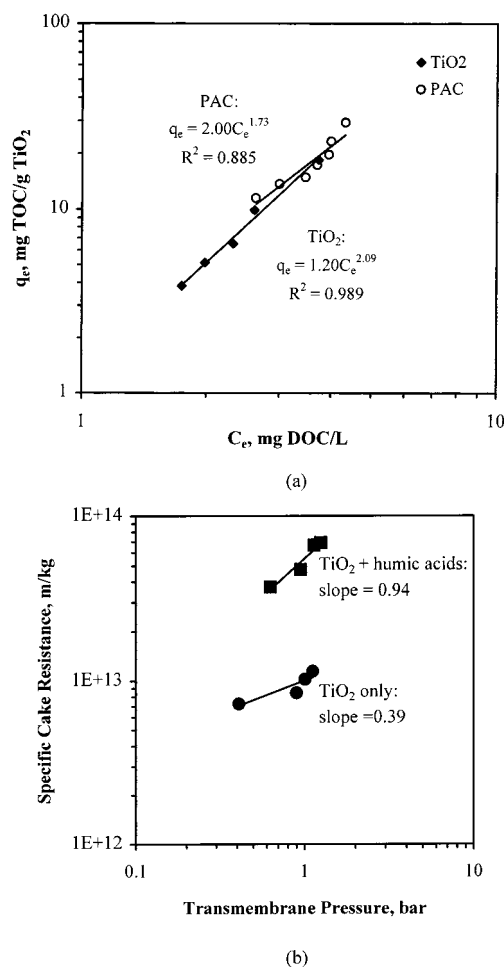


Figure 6. Nature of TiO₂ particles and their cakes: (a) adsorption isotherm of humic acids on TiO₂ (this work) and PAC (obtained from ref 19), (b) specific cake resistance and cake compressibility (slope) of TiO₂ particles alone and of a mixture of TiO₂ particles and humic acids.

regardless of the flow conditions and their sequence. The initial flux decline at the higher cross-flow velocity was still significant because the flux was already so high that most of the TiO₂ particles could move onto the membrane surface, as shown in Figure 4. Also, no flux improvement was achieved at the high cross-flow velocity of 1 m/s after the membrane had previously been fouled by operation for an extended period of time at low cross-flow velocities. Overall, the patterns in flux decline seemed very similar under the two different flow sequences used, although the initial flux decline at a cross-flow velocity of 0.25 m/s was a bit greater than that at the higher velocity.

However, the UV absorbance (UV₂₅₄) of the permeate at 254 nm varied greatly with the change in flow conditions (Figure 7b), although there was a trend in UV₂₅₄ of the permeate. It appears that the higher the fluid velocities, the lower the UV₂₅₄ of the permeate. The trend in UV₂₅₄ removal at different velocities can be explained by three possible causes, namely, adsorption kinetics, particle size changes, and concentration polarization. First, the variation in UV₂₅₄ in the permeate was monitored with time to examine the kinetic effect of humic acid adsorption onto TiO₂ particles. The UV₂₅₄ of the permeate reached a steady state within 30 min, suggesting that adsorption was completed rapidly. Furthermore, in Figure 7b, the increase in UV₂₅₄ with the stepwise decrease in fluid velocity with time also

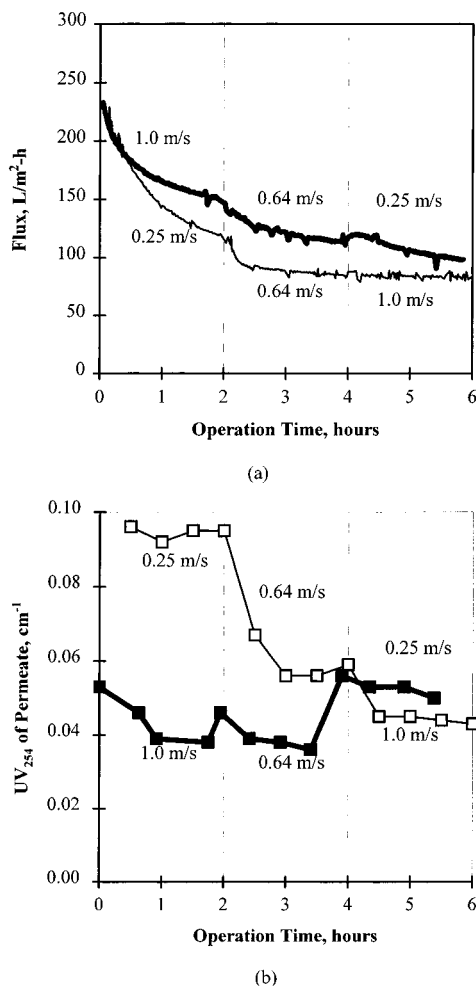


Figure 7. Variation in (a) permeate flux and (b) UV_{254} of permeate when cross-flow velocities are changed with time; UV_{254} of feed = 0.300 cm^{-1} .

indicates that the kinetics could not be responsible for the variation in the UV_{254} of the permeate. Second, a reduction in particle size at higher velocities was possible because of the higher shear rates and might provide a larger surface area for adsorption. Therefore, the particle size distribution and SEM images of the particles were measured to identify the change in TiO_2 particle size. However, there was no noticeable change in particle size at different fluid velocities. Finally, the accumulation of humic acids at the membrane surface should be considered because the higher concentration of humic acids by concentration polarization could provide a larger driving force for humic acids to pass through the membrane. In contrast, the larger fluid velocity could prevent humic acids from polarizing at the membrane surface by shear. Thus, the ratio of the wall concentration (C_w) to the bulk concentration (C_b) for the partially retentive membrane was calculated using eq 3 based on the film theory model²¹ and the actual flux data given in Figure 7a. The ratios are displayed in Figure 8.

$$\frac{C_w - C_p}{C_b - C_p} = \exp\left(\frac{J}{k}\right) \quad (3)$$

Here, C_p is the permeate concentration of humic acids, J is the permeate flux, and k is the mass transfer

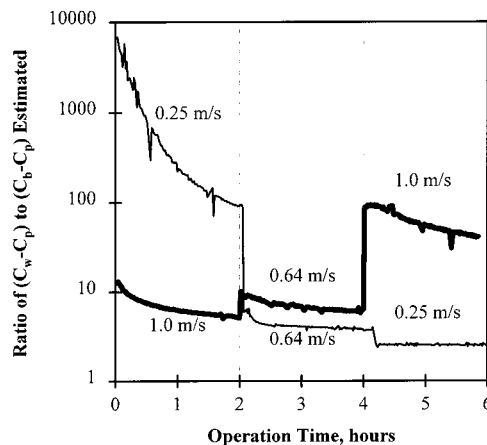


Figure 8. Estimate of the degree of concentration polarization with time at different cross-flow velocities using eq 3; average diffusivity of humic acids = $4.82 \times 10^{-10} \text{ m}^2/\text{s}$.

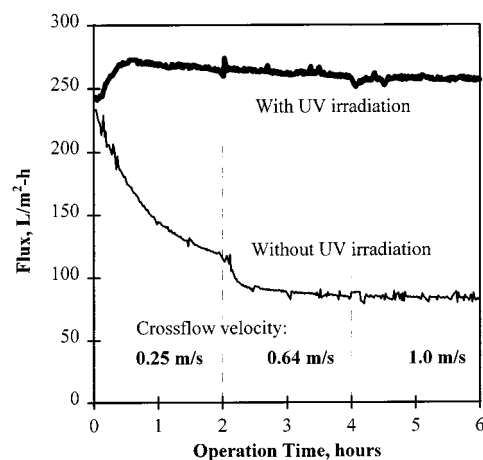


Figure 9. Effect of UV irradiation (photocatalysis) on UF flux.

coefficient that was calculated using the equations given below.²²

For laminar flow

$$Sh = \frac{k d_h}{D} = 1.62 \left(Re Sc \frac{d_h}{L} \right)^{0.33} \quad (4)$$

For turbulent flow

$$Sh = \frac{k d_h}{D} = 0.023 Re^{0.8} Sc^{0.3} \quad (5)$$

where Sh is the Sherwood number (dimensionless), d_h is the equivalent hydraulic diameter (m), Re is the Reynolds number (dimensionless), Sc is the Schmidt number (dimensionless), and L is the membrane channel length (m).

A similar trend was observed between the permeate UV_{254} and the ratio at different flow conditions (compare Figures 7b and 8). The concentration gradient at the membrane surface decreased when the flow was transformed from laminar to turbulent, which interfered with the passage of humic acids through the membrane. Consequently, it is believed that the cross-flow velocities had a strong influence on the UV_{254} removal because of the concentration polarization effect of humic acids at the membrane surfaces.

Effect of UV Irradiation. Figure 9 compares the UF flux for a mixture of humic acids and TiO_2 particles with and without UV irradiation. When photocatalytic reac-

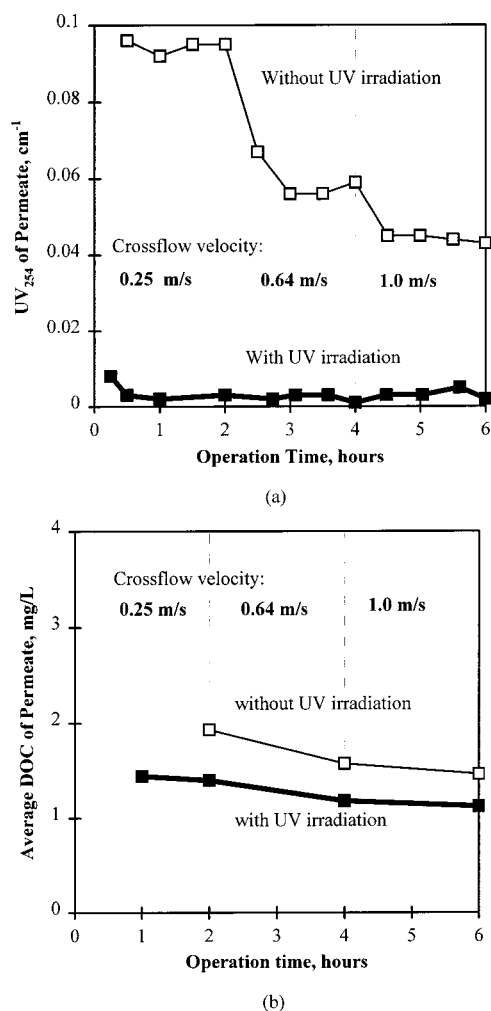


Figure 10. Effect of UV irradiation on (a) UV₂₅₄ and (b) DOC removal.

tions occurred with UV irradiation, no flux decline was observed during the 6-h operations. This result could be associated with the photocatalytic degradation of humic acids under UV irradiation.²³ As shown in Figure 10a, the UV₂₅₄ of the permeate with UV irradiation was maintained at a very low level of below 0.009 cm⁻¹. As discussed above, the flux decline for the mixed system was caused by the accumulation of highly compressible humic-acid-laden TiO₂ particles at the membrane. Thus, the degradation of humic acids present in suspension or bound to the TiO₂ particle surfaces must play a central role in the improvement of the flux when UV irradiation was provided.

Interestingly, however, the difference in permeate DOC between samples with and without UV irradiation was fairly small compared with the difference in the UV₂₅₄, that is, with UV irradiation, the average removal efficiencies for DOC increased by less than 10% (from 59 to 68%), even though the UV removal efficiency was raised by more than 20%. This indicates that the humic acids were not completely mineralized with UV irradiation and photocatalysis but that the aromatic structure of the humic acids was partially broken or changed to different forms with less-adsorptive properties. Overall, photocatalytic reactions appear to be attractive for the control of membrane fouling and removal of humic acids during the UF of TiO₂ particles in the presence of fouling materials such as natural organic matter.

Conclusions

In this study, the use of ultrafiltration for the separation of TiO₂ photocatalysts that were used for drinking water treatment was investigated. The effect of natural organic matter (i.e., humic acids) and cross-flow velocities on UF fluxes and organic removal was evaluated with and without photocatalytic reactions. The following conclusions can be drawn:

(1) When the UF of TiO₂ particles was carried out in the presence of humic acids without UV irradiation, the flux decline was relatively substantial because of the formation of denser cake layers with humic-acid-laden TiO₂ particles. A theoretical approach to the back-transport of TiO₂ particles and humic acids helped to explain the significance of the adsorption of humic acids onto photocatalysts, and its contribution to the higher cake resistance was confirmed by the measurement of the adsorption capacity and specific cake resistance.

(2) The removal efficiencies for UV₂₅₄ increased when the cross-flow velocities became higher. This was because the concentration polarization of humic acids at the membrane surface was inhibited by the higher shear rates and, consequently, the driving force for the passage of humic acids was reduced. Accordingly, it was found that cross-flow velocities were an important operating factor affecting permeate quality.

(3) There was no flux reduction with photocatalytic degradation of humic acids, and moreover, the UV₂₅₄ removal of the permeate was achieved at a level of approximately 97–99%. However, there was a slight difference in DOC removal, that is, humic acids were not completely oxidized to CO₂ by photocatalytic reactions but were transformed to other forms that have little UV absorption. In summary, photocatalytic reactions with UV irradiation were effective in improving the membrane flux while changing the chemical forms of the humic acids, but DOC removal was not as effective as flux enhancement. A UF process is potentially an attractive method for the separation of photocatalysts from drinking water without any concerns about membrane fouling as long as photocatalytic reactions are occurring.

Acknowledgment

The authors thank the Korea Science and Engineering Foundation for their financial support under Grant 98-05-2-03-01-3.

Literature Cited

- (1) Dionysiou, D. D.; Suidan, M. T.; Bekou, E.; Baudin, I.; Laine, J. M. Effect of Ionic Strength and Hydrogen Peroxide on the Photocatalytic Degradation of 4-Chlorobenzoic Acids in Water. *Appl. Catal. B* **2000**, *26*, 153.
- (2) Kagaya, S.; Shimizu, K.; Arai, R.; Hasegawa, K. Separation of Titanium Dioxide Photocatalyst in Its Aqueous Suspensions by Coagulation with Basic Aluminum Chloride. *Water Res.* **1999**, *33*, 1753.
- (3) Selli, E.; Baglio, D.; Montanarella, L.; Bidoglio, G. Role of Humic Acids in the TiO₂-Photocatalyzed Degradation of Tetrachloroethene in Water. *Water Res.* **1999**, *33*, 1827.
- (4) Tennakone, K.; Tilakaratne, C. T. K.; Kottegoda, I. R. M. Photocatalytic Degradation of Organic Contaminants in Water with TiO₂ Supported on Polythene Films. *J. Photochem. Photobiol. A* **1995**, *87*, 177.
- (5) Robert, D.; Gauthier, A. Prospects for a Supported Photocatalyst in the Detoxification of Drinking Water. *Water Qual. Int.* **1998**, Nov/Dec, 27.

- (6) Molinari, R.; Mungari, M.; Drioli, E.; Paola, A. D.; Loddo, V.; Palmisano, L.; Schiavello, M. Study on a Photocatalytic Membrane Reactor for Water Purification. *Catal. Today* **2000**, *55*, 71.
- (7) Schmelling, D. C.; Gray, K. A.; Kamat, P. V. The Influence of Solution Matrix on the Photocatalytic Degradation of TNT in TiO₂ Slurries. *Water Res.* **1997**, *31*, 1439.
- (8) Pruden, A. L.; Ollis, D. H. Photoassisted Heterogeneous Catalysis: The Degradation of Trichloroethylene in Water. *J. Catal.* **1983**, *82*, 404.
- (9) Ollis, D. F.; Hsiao, C.; Budiman, L.; Lee, C. Heterogeneous Photoassisted Catalysis: Conversions of Perchloroethylene, Dichloroethane, Chloroacetic Acids and Chlorobenzenes. *J. Catal.* **1984**, *88*, 89.
- (10) Minero, C.; Pelizzetti, E.; Sega, M.; Friberg, S. E.; Sjöblom, J. The Role of Humic Substances in the Photocatalytic Degradation of Water Contaminants. *J. Dispersion Sci. Technol.* **1999**, *20*, 643.
- (11) Bems, B.; Jentoft, F. C.; Schlögl, R. Photoinduced Decomposition of Nitrate in Drinking Water in the Presence of Titania and Humic Acids. *Appl. Catal. B* **1999**, *20*, 155.
- (12) Richardson, S. D.; Thruston, A. D.; Collette, T. W.; Patterson, K. S.; Lykins, B. W.; Ireland, J. C. Identification of TiO₂/UV Disinfection Byproducts in Drinking Water. *Environ. Sci. Technol.* **1996**, *30*, 3327.
- (13) Eggins, B. R.; Palmer, F. L.; Byrne, J. A. Photocatalytic Treatment of Humic Substances in Drinking Water. *Water Res.* **1997**, *31*, 1223.
- (14) Sopajaree, K.; Qasim, S. A.; Basak, S.; Rajeshwar, K. An Integrated Flow Reactor–Membrane Filtration System for Heterogeneous Photocatalysis Part I: Experiments and Modeling of a Batch-Recirculated Photoreactor. *J. Appl. Electrochem.* **1999**, *29*, 533.
- (15) Sopajaree, K.; Qasim, S. A.; Basak, S.; Rajeshwar, K. An Integrated Flow Reactor–Membrane Filtration System for Heterogeneous Photocatalyst Part II: Experiments on the Ultrafiltration Unit and Combined Operation. *J. Appl. Electrochem.* **1999**, *29*, 1111.
- (16) Choo, K. H.; Lee, C. H. Hydrodynamic Behavior of Anaerobic Biosolids during Crossflow Filtration in the Membrane Anaerobic Bioreactor. *Water Res.* **1998**, *32*, 3387.
- (17) Almann, J.; Ripperger, S. Particle Deposition and Layer Formation at the Crossflow Microfiltration. *J. Membr. Sci.* **1997**, *124*, 119.
- (18) Cheryan, M. *Ultrafiltration and Microfiltration Handbook*; Technomic Publishing Co.: Lancaster, PA, 1998.
- (19) Lee, S. J. Removal of Trace Organics and Humic Acids in a PAC–UF System. M.Sc. Thesis, Seoul National University, Seoul, Korea, 1997.
- (20) Lee, S. J.; Choo, K. H.; Lee, C. H. Conjunctive Use of Ultrafiltration with Powdered Activated Carbon Adsorption for Removal of Synthetic and Natural Organic Matter. *J. Ind. Eng. Chem.* **2000**, *6*, 356.
- (21) Mulder, M. *Basic Principles of Membrane Technology*; Kluwer Academic Publishers: Dordrecht, The Netherlands, 1996.
- (22) Porter, M. C. Concentration Polarization with Membrane Ultrafiltration. *Ind. Eng. Chem. Prod. Res. Dev.* **1972**, *11*, 234.
- (23) Bekbölet, M.; Özköşemen, G. A. Preliminary Investigation on the Photocatalytic Degradation of a Model Humic Acid. *Water Sci. Technol.* **1996**, *33*, 189.

Received for review August 9, 2000

Revised manuscript received January 8, 2001

Accepted January 12, 2001

IE000738P